ENPM640 Project
Adaptive Impedance Control Applied to Robot-Aided Neuro-Rehabilitation of the Ankle

Aditya Varadaraj
UID: 117054859
University of Maryland
College Park, USA

Saurabh Palande
UID: 118133959
University of Maryland
College Park, USA

Jeffin Johny
UID: 118293929
University of Maryland
College Park, USA

Prateek Verma
UID: 118435039
University of Maryland
College Park, USA

***Abstract*—With an increasingly aging population, the demand for post-stroke therapy is likely to rise and rehabilitation robots can play a vital role in recovery. An assistive-resistive approach was implemented in the main paper to promote active patient participation during robotic therapy. The robotic assistance was implemented in real-time according to the instantaneous patient's participation and performance. The robot used for this purpose was an Anklebot, where the patient played a game while sitting. Both adaptive and fixed-stiffness approach was compared in the main paper and it was found that the adaptive approach provides more kinematic variability in patient-led movements, without compromising overall performance. Most of the results from the main paper were validated by simulating the virtual ankle stiffness values of the human obtained during the game. Furthermore, the cost function from the main paper was modified for enhancement 1 by replacing L2 error by L1 error for adaptive stiffness calculation, and force feedback control was added to decrease the apparent mass and friction felt by the human due to the robot. The efficacy of the enhancements has been showcased.**

***Index Terms*—assistive-resistive, force feedback, rehabilitation robots**

I. Introduction

Stroke is a major health problem, where the blood arteries in the brain are ruptured and can have devastating consequences. Stroke generally damages neural areas that control the movement of both upper and lower limbs. And recent studies have found that stroke risk has gone high in young adults as well [8]. While the statistics [10] seem to be alarming, it should be noted that stroke survivors are able to regain almost full mobility with proper physiotherapy [9]. But with the predicted increase in the number of patients, physiotherapists would not be able to deliver proper assistance to all. This is the main focus of rehabilitation robots so that more patients would be able to get therapy and would have better results than what they get solely from human therapists.

Significant developments have taken place in the field of robot-aided rehabilitation in the past few decades. Robotic systems for rehabilitation purposes are designed with the intent of evoking neural plasticity and muscle activation synergies through specific repetitive motor coordination exercises.

"Assist-as needed" approaches consist of providing the appropriate amount of external assistance for the patient to complete an exercise regime when he/she cannot complete it. [11]. There are Resistive approaches that provide resistance to build up the core strength of the impaired limb as the patient has to apply more effort to complete a task [12]. Both upper-limb and lower-limb rehabilitation devices were developed but recently more focus has been on lower-body rehabilitation as its important for gait.

The Ankle is the most substantial part of the human gait as it provides propulsion for walking and absorbs shock while jumping. The robot used in this paper is the Anklebot, [17] where the patients attempted dorsi/plantarflexion movements while in a seated position. This type of setup is useful for patients who still haven't regained the ability to stand on foot. The stroke timeline for these patients would be generally in the subacute phase.

In the following section, a brief overview of the relevant literature in the field of rehabilitation robots is presented. Section III deals with the derivations of equations of the control law and kinematics from the main paper. A detailed description of the implemented enhancements is done in section IV. Sections V and VI, showcase the simulation results and the conclusion drawn between the existing approach and proposed enhancements, respectively.

II. Literature Review

In the beginning, robotic actuation was designed using heavy actuation devices with stiff position/velocity and torque control methods. The transmission mechanisms were also rigid and non back-drivable [13]. This would work without any issue if there is no external disturbance and if the working environment is well-defined. But an impaired human is a high source of noise and the coupled system can be destabilized which can cause fatal injury to the patient if he/she falls down. The above problem can be solved if the environmental factor is taken into account, and provide some form of autonomy for the patient.

Impedance control solves most of the issues [14], it promotes active participation of the patient as assistance is only

provided when the patient deviates from desired trajectory. Various variants of impedance control have been implemented. For instance, in a performance-based controller, [15], the robot guides the patient through a virtual tunnel along a minimum jerk trajectory. The tunnel serves as a boundary and patients can freely move inside the determined boundary of the tunnel, which is modified over time to improve patient performance. Kinematic and kinetics metrics have been proposed as valid measures of motor recovery for rehabilitation robots [16].

The idea implemented by the main paper was that, [1], depending on patient participation and performance, the robot actuation shifts smoothly between assistance and resistance. Their prior works [3] and [4] included the computation of cost function to optimize the robot behavior, where the cost depended upon the assistive force exerted by the robot on the patient and the patient motion error. For their experiments they used Anklebot. The anklebot [17] can apply up to 23 N/m in DP. The weight of the user cannot be supported, however, these torques can properly position the ankle during the swing phase and assist during toe-off and heel-strike gait phases, minimizing foot drop and foot slap in stroke patients.

III. Control proposed in the paper

A. Adaptive Stiffness Impedance Control

1) Estimation of Patient Participation: Human-robot dynamics in the dorsi/plantarflexion degree of freedom can be modeled by:

$$\tau_r + \tau_h = M\ddot{\theta} + C\dot{\theta} + G(\theta) \tag{1}$$

where θ denotes the sagittal angular position of the ankle joint;M, C and G are, respectively, inertial, velocity-dependent and gravitational matrices and, τ_r and τ_h are torques exerted by robot and patient, respectively. The M matrix which is

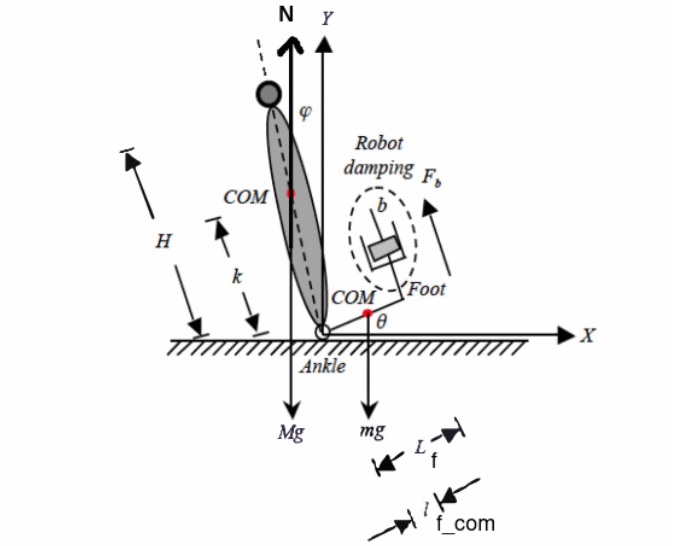

Fig. 1. AnkleBot FBD diagram [2]

inertia of the foot about the ankle is given by

$$M = \frac{M_f l_f^2}{3} \tag{2}$$

As can be seen in experimental setup shown in Fig. 2, and

Fig. 2. Anklebot Experimental Setup [1]

as mentioned in [1], the legs and calves, i.e., everything other than the foot are supported by the barber-like chair including the anklebot. Thus, the only gravitational torque will be acting on the center of mass of the foot. Calculating the torques about the ankle, from Fig. 1, we get:

$$G(\theta) = -M_f g l_{f,com} cos\theta \tag{3}$$

The velocity-dependent C matrix is only due to the damping of human and robot. From this we get:

$$C = B_h + B_r \tag{4}$$

Assuming that the individual is controlling the mechanical impedance of his/her ankle to follow a virtual trajectory, the ankle's dynamics can be modeled by a 1st-order relation between angular position and human torque

$$\tau_h = K_h(\theta_{eq} - \theta) - B_h\dot{\theta} \tag{5}$$

where K_h and B_h are, respectively, stiffness and damping of the inner human control, and θ_{eq} is an equilibrium angle. Similarly, the robot torque is given by:

$$\tau_r = K_r(\theta_d - \theta) - B_r\dot{\theta} + \tau_e \tag{6}$$

where θ_d is a desired angular position according to the robot's reference trajectory, and K_r and B_r are, respectively, the stiffness and damping of the impedance controller and, τ_e is the resistive torque, kept constant in the paper and our simulations.

In order to identify the purported patient participation, the ankle stiffness K_h needs to be estimated. Considering equation (1), (5) and (6) and assuming $\theta_d = \theta_{eq}$ we get,

$$K_h(\theta_{eq}-\theta) - B_h\dot{\theta} + K_r(\theta_d-\theta) - B_r\dot{\theta} + \tau_e = M\ddot{\theta} + C\dot{\theta} + G(\theta) \tag{7}$$

Taking $\theta_e = \theta_d - \theta$ as the position error,

$$K_h\theta_e - B_h\dot{\theta} + K_r\theta_e - B_r\dot{\theta} + \tau_e = M\ddot{\theta} + C\dot{\theta} + G(\theta)$$

$$K_h = \frac{M\ddot{\theta} + (B_h + B_r + C)\dot{\theta} + G - \tau_e - K_r\theta_e}{\theta_e}$$

$$\hat{K_h} = \frac{M\ddot{\theta} + H\dot{\theta} + G - \tau_e}{\theta_e} - K_r \tag{8}$$

where $H = B_h + B_r + C$ In the original paper, experiments (goal is to find motor torques) are performed and the value of θ and $\dot{\theta}$ are recorded using sensors and using these values K_h is calculated. Since we are doing simulation (goal is to solve the equations to get θ and $\dot{\theta}$), hence K_h is produced synthetically to approximate patient's response similar to the paper.

2) Optimal Robot Stiffness: To optimize the robot actuation, a cost function needs to be minimized that weighs a metric of accuracy (the position error) and a metric of effort (the robotic assistance torque). The cost function is given by:

$$J = \theta_e^2 + \beta\tau_r^2 \tag{9}$$

To find the optimal value of K_r that optimizes J we differentiate J with respect to K_r

$$\frac{\partial J}{\partial K_r} = 2\theta_e\frac{\partial \theta_e}{\partial K_r} + 2\beta\tau_r\frac{\partial \tau_r}{\partial K_r} \tag{10}$$

Now, $\frac{\partial \theta_e}{\partial K_r}$ is calculated from equation (8)

$$\frac{\partial \theta_e}{\partial K_r} = -\frac{M\ddot{\theta} + H\dot{\theta} + G - \tau_e}{(K_r + \hat{K_h})^2}$$

$$\frac{\partial \tau_r}{\partial K_r} = \theta_e + K_r\frac{\partial \theta_e}{\partial K_r}$$

Substituting the value of $\frac{\partial \theta_e}{\partial K_r}$ and $\frac{\partial \tau_r}{\partial K_r}$ in equation (10) and equating it to zero, we get

$$2\theta_e\frac{\partial \theta_e}{\partial K_r} + 2\beta\tau_r(\theta_e + K_r\frac{\partial \theta_e}{\partial K_r}) = 0$$

$$\beta\tau_r\theta_e = -\frac{\partial \theta_e}{\partial K_r}(\theta_e + \beta\tau_r K_r)$$

$$\beta\tau_r\theta_e = (\theta_e + \beta\tau_r K_r)\frac{M\ddot{\theta} + H\dot{\theta} + G - \tau_e}{(K_r + \hat{K_h})^2}$$

$$\beta\tau_r(K_r + \hat{K_h})^2 = (\theta_e + \beta\tau_r K_r)\frac{M\ddot{\theta} + H\dot{\theta} + G - \tau_e}{\theta_e}$$

$$\beta\tau_r(K_r + \hat{K_h})^2 = (\theta_e + \beta\tau_r K_r)(K_r + \hat{K_h})$$

$$\beta\tau_r(K_r + \hat{K_h}) = \theta_e + \beta\tau_r K_r$$

$$\theta_e = \hat{K_h}\beta\tau_r \tag{11}$$

Considering steady state (as in [3], [4]) and taking τ_e to be zero in equation (6) we get,

$$K_r = \frac{\tau_r}{\theta_e}$$

The optimal value of Robot stiffness is:

$$K_r^* = \frac{1}{\beta\hat{K_h}} \tag{12}$$

In order to establish an upper limit for the robot stiffness when the patient does not participate during a given movement ($K_r^* = \infty$) the final value of K_r is bounded by:

$$K_r^a = min\{K_r^c, K_r^*\}$$

where K_r^c is the robot stiffness necessary to reach an admissible error θ_e^{adm} defined as:

$$K_r^c = \frac{G(\theta) - \tau_e}{\theta_e^{adm}}$$

3) Performance Based Adaptation: If patient does not participate during consecutive movements ($K_h - > 0$), the robot will increase its stiffness until reaching the maximum value allowed in an attempt to complete the movement within an error threshold. At the same time, it is expected that the patient will optimize his/her effort, reducing his/her participation. In order to promote the necessary patient participation, the practical robot stiffness, K_r , is limited by:

$$\bar{K_r} = \alpha K_r^a \tag{13}$$

where $0 \leq \alpha \leq 1$ is an assistance factor adapted at each movement by the following performance-based adaptive strategy:

$$\alpha_{k+1} = f\alpha_k + gP_k \tag{14}$$

where k is a temporal index for movements, f and g are forgetting and gain factors, respectively, and Pk is an error-based performance measurement given by $P_k = E/E_{max}$, where E is the sum of the error during the movement. The value of $\bar{K_r}$ found is used to calculate τ_r from equation (6)

B. Fixed Stiffness Impedance Control

In case of Fixed Stiffness Impedance Control, the step of estimating the patient participation remains same as in the case of Adaptive Stiffness and all the equations used in that section remains valid.

The value of $\bar{K_r}$ is defined as a constant value of 125 Nm/rad. This constant value of $\bar{K_r}$ is used to calculate τ_r from equation (6)

IV. ENHANCEMENTS

We made 2 major enhancements to the control system proposed in the paper.

A. Enhancement 1: Using L1 Error Cost Function

In the equation given for cost J in previous section (Eq. (9)), we can see that it is the sum of the L2 error θ_e^2 in DP Angle θ with a regularization term $\beta\tau_r^2$ which ensures that robot contribution is minimized (human effort is maximized) simultaneously.

The first enhancement we performed was to replace the L2 error θ_e^2 with L1 error, i.e., $|\theta_e|$.

$$\begin{aligned} J &= |\theta_e| + \beta\tau_r^2 \\ \frac{\delta J}{\delta K_r} &= \frac{\theta_e}{|\theta_e|}\frac{\delta\theta_e}{\delta K_r} + 2\beta\tau_r\frac{\delta\tau_r}{\delta K_r} \\ \textit{As derived earlier, } \frac{\delta\theta_e}{\delta K_r} &= -\frac{(M\ddot{\theta} + H\dot{\theta} + G - \tau_e)}{(K_h + K_r)^2} \\ \textit{and } \frac{\delta\tau_r}{\delta K_r} &= \theta_e - \frac{K_r(M\ddot{\theta} + H\dot{\theta} + G - \tau_e)}{(K_h + K_r)^2} \\ \textit{, where, } H &= C + B_h + B_r \\ \textit{and } C &= B_h + B_r \end{aligned} \tag{15}$$

$$\begin{aligned} \Rightarrow \frac{\delta J}{\delta K_r} &= \frac{\theta}{|\theta_e|}\left(-\frac{(M\ddot{\theta} + H\dot{\theta} + G - \tau_e)}{(K_h + K_r)^2}\right) \\ &+ 2\beta\tau_r\left(\theta_e - \frac{K_r(M\ddot{\theta} + H\dot{\theta} + G - \tau_e)}{(K_h + K_r)^2}\right) \\ &= \left(\frac{\theta}{|\theta_e|} + 2\beta\tau_r K_r\right)\left(-\frac{(M\ddot{\theta} + H\dot{\theta} + G - \tau_e)}{(K_h + K_r)^2}\right) \\ &+ 2\beta\tau_r\theta_e \\ &= 0 \end{aligned} \tag{16}$$

Thus, we get:

$$\begin{aligned} &\left(\frac{\theta}{|\theta_e|} + 2\beta\tau_r K_r\right)\left(\frac{(M\ddot{\theta} + H\dot{\theta} + G - \tau_e)}{\theta_e}\right) \\ &= 2\beta\tau_r(K_h + K_r)^2 \\ &\left(\frac{\theta}{|\theta_e|} + 2\beta\tau_r K_r\right)(K_h + K_r) = 2\beta\tau_r(K_h + K_r)^2 \\ &\frac{\theta}{|\theta_e|} + 2\beta\tau_r K_r = 2\beta\tau_r K_h + 2\beta\tau_r K_r \\ &\tau_r = \frac{\theta_e}{2\beta K_h|\theta_e|} \\ &\textit{Assuming Steady State Conditions,} \\ &\tau_r = K_r\theta_e \\ &K_r^* = \frac{\tau_r}{\theta_e} = \frac{1}{2\beta K_h|\theta_e|} \end{aligned} \tag{17}$$

We use this value of Kr^* and do calculations similar to adaptive impedance controller explained in previous section.

B. Enhancement 2: Adding Force Feedback

For the second enhancement, we add Force Feedback to the System keeping the original L2 error cost function. The control block diagram is shown in Fig. 3

The control law and equations of motion are given in Eq. (18).

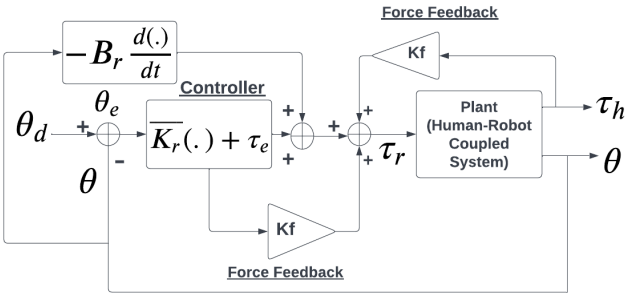

Fig. 3. Adaptive Stiffness Impedance Control with Force Feedback

$$\begin{aligned} \tau_h &= K_h\theta_e - B_h\dot{\theta} \\ \tau_r &= K_r\theta_e - B_r\dot{\theta} + \tau_e + K_f(K_r\theta_e - B_r\dot{\theta} + \tau_e + \tau_h) \\ \tau_r + \tau_h &= M\ddot{\theta} + C\dot{\theta} + G(\theta) \end{aligned} \tag{18}$$

Combining above equations, we get:

$$\begin{aligned} &(1 + K_f)K_r\theta_e - (1 + K_f)B_r\dot{(\theta)} + (1 + K_f)\tau_e \\ &+ K_f\tau_h + K_h\theta_e - B_h\dot{\theta} \;=\; M\ddot{\theta} + C\dot{\theta} + G \\ &\Rightarrow (1 + K_f)K_r\theta_e - (1 + K_f)B_r\dot{\theta} + (1 + K_f)\tau_e \\ &+ (1 + K_f)K_h\theta_e - (1 + K_f)B_h\dot{\theta} \;=\; M\ddot{\theta} + C\dot{\theta} + G \end{aligned} \tag{19}$$

$$\begin{aligned} \theta_e &= \frac{M\ddot{\theta} + (C + (1 + K_f)(B_h + B_r))\dot{\theta} + G - (1 + K_f)\tau_e}{(1 + K_f)(K_r + K_h)} \\ \textit{Let } \eta &= M\ddot{\theta} + (C + (1 + K_f)(B_h + B_r))\dot{\theta} + G - (1 + K_f)\tau_e \\ \frac{d\theta_e}{dK_r} &= \frac{-\eta(1 + K_f)}{((1 + K_f)(K_h + K_r))^2} \end{aligned} \tag{20}$$

Now, we minimize the cost given below:

$$\begin{aligned} J &= \theta_e^2 + \beta\tau_r^2 \\ \nabla_{K_r}J &= 2\theta_e\frac{d\theta_e}{dK_r} + 2\beta\tau_r\frac{d\tau_r}{dK_r} \end{aligned} \tag{21}$$

Substituting result of Eq. (20), we get:

$$\begin{aligned} &\nabla_{K_r}J = (2\theta_e + 2\beta(1 + K_f)\tau_r K_r)\left(\frac{-\eta(1 + K_f)}{((1 + K_f)(K_h + K_r))^2}\right) \\ &+ 2\beta(1 + K_f)\tau_r\theta_e \;=\; 0 \\ &2\beta\tau_r((1 + K_f)(K_h + K_r))^2 \\ &=\; (2\theta_e + 2\beta(1 + K_f)\tau_r K_r)((1 + K_f)(K_h + K_r)) \\ &\Rightarrow \theta_e \;=\; \beta(1 + K_f)\tau_r K_h \\ &\Rightarrow \frac{\tau_r}{\theta_e} \;=\; \frac{1}{\beta(1 + K_f)} \end{aligned} \tag{22}$$

Assuming Steady State Conditions, i.e., $\ddot{\theta} = \dot{\theta} = 0$, we get:

$$\begin{aligned} \tau_r &= (1+K_f)K_r\theta_e + K_f\tau_h \\ \Rightarrow\ K_r^* &= \frac{\tau_r - K_f\tau_h}{(1+K_f)\theta_e} \\ &= \frac{1}{\beta(1+K_f)^2K_h} - \frac{K_f\tau_h}{(1+K_f)\theta_e} \\ K_r^* &= \frac{1}{\beta(1+K_f)^2K_h} - \frac{K_fK_h}{(1+K_f)} \end{aligned} \tag{23}$$

After this, we follow same equations as used in Adaptive Stiffness Impedance Control to find $\bar{K}_r$ from K_r^* and use it in Eq (18) to find θ and $\dot{\theta}$ by solving the ODE using Python's **scipy.integrate.odeint()** which uses the RK-45 (Runge Kutta) numerical integration method.

Rearranging Eq. (19), we get:

$$\begin{aligned} &\frac{M}{(1+K_f)}\ddot{\theta} + \frac{C}{(1+K_f)}\dot{\theta} + \frac{G}{(1+K_f)} \\ &- K_r\theta_e + B_r\dot{\theta} - \tau_e \ =\ K_h\theta_e - B_h\dot{\theta} \end{aligned} \tag{24}$$

Thus, from Eq. (24), we realize that for $K_f \in [0, 1]$, we get **reduced equivalent inertia and damping** while keeping the system passive.

V. Experimental Setup

A. Subject Information

The experimental setup is based on the Anklebot system. A simulation environment based on Python programming language is being defined for this setup. The subjects are defined by pre-generated input signals where the proposed control scheme is provided with the following parameters: Height of the subject is taken as 169 cms and the weight is taken as 83.6 kgs. These are the maximum values for height and weight mentioned in the reference paper [1].

B. Experimental Protocol

The setup deviced in the reference paper is the Anklebot wore by the subjects while sitting on a barber-like chair and the trials include 40 unassisted alternating movements (20 Dorsiflexions and 20 Plantarflexions). In our simulation, we perfomred the movements for 80 unassisted alternating movements to generate the end results. The code has the provision to take the number of movements as user input by modifying the "n_movements" variable. The experimetal setup is defined so that we measure the patient's performance while s/he is playing a computational game and modify the level of the robotic assistance during the movement. Simulteneously, We analyze pilot outcomes using this adaptive method with a fixed-stiffness impedence control, adaptive stiffness impedance control, adaptive stiffness impedance control with L1 error cost function and adaptive stiffness impedance control with force-feedback.

C. Parameters used in the simulation

Mass of the foot, $M_f = 0.0145M_{body} = 1.2122\ kg$ [7]
Length of foot, $l_f = 0.152H_{body} = 0.2569\ meters$ [18]
Damping parameter of robot, $B_r = 1\ Nms/rad$
Ankle Damping, $B_h = 0.03M_{body} = 2.51Nms/rad$
As per [1], $\beta = 0.0005$; Forgetting factor, $f = 0.9$
Gain factor $g = 0.1$; $\theta_e^{adm} = 1.4^o$
Initial value of $\alpha = 1$; Target positions, $\theta_t = \pm 7^o$ Initial values of θ are -7.5 degrees for dorsiflexion and +7.5 degrees for plantarflexion.
Initial values of $\dot{\theta} = 0$ and $\ddot{\theta} = 0$
The Stiffness K_h(from human participation) is taken from an exponential distribution to mimic the data produced by the subjects in the paper:
For the fixed stiffness case, $\bar{K}_r = 125\ Nm/rad$
The force-feedback gain is taken as $K_f = 0.1$ in the simulation for the second enhancement. The reference trajectory for 3 secs, i.e., one movement is given by:

$$\theta_d = \begin{cases} \theta_l \left[\dfrac{20t^3 - 15t^4 + 3t^5}{16}\right] + \theta_{t_{i-1}} & if\ 0 < t < 2 \\ \theta_{t_i} & if\ 2 \le t \le 3 \end{cases} \tag{25}$$

, where, $\theta_l = \theta_{t_i} - \theta_{t_{i-1}}$, where, θ_{t_i} and $\theta_{t_{i-1}}$ are current and previous targets respectively.

VI. Results

A. Fixed Stiffness

Here, we have taken robot gain as $\bar{K}_r = 125\ Nm/rad$. The results are shown in Fig.4.

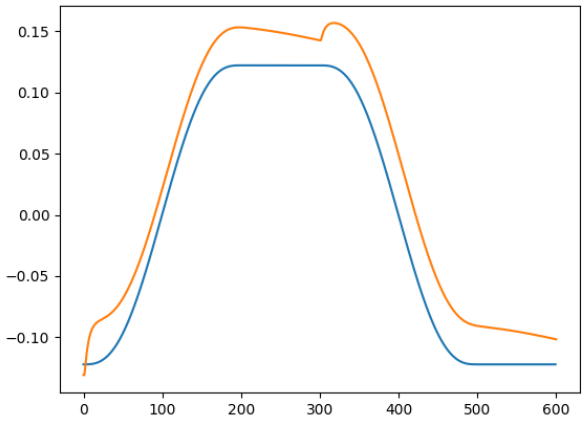

Fig. 4. Plot of θ for two movements for fixed stiffness impedence control

B. Adaptive Stiffness

Here, we adjust the value of $\bar{K}_r$ based on patient participation. The results are shown in Fig.5 and Fig.6.

We observed that the adaptive-stiffness approach preserves the main features of the impedance control and allows more

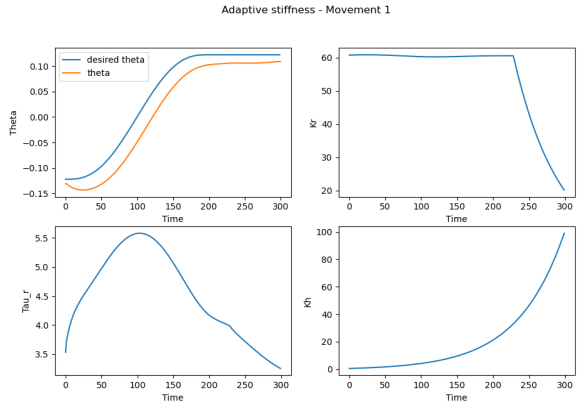

Fig. 5. Plot of a) θ, b) K_r, c) τ_r, and d) K_h for dorsiflexion for adaptive stiffness impedence control

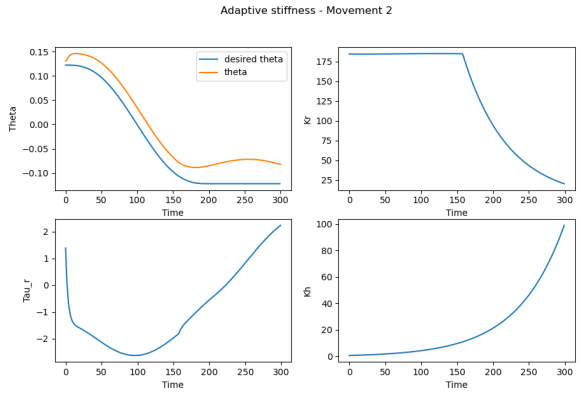

Fig. 6. Plot of a) θ, b) K_r, c) τ_r, and d) K_h for plantarflexion for adaptive stiffness impedence control

kinematic variability in motions led by patient, smoothly increasing the task difficulty as a function of the participation.

C. Enhancement 1 (Using L1 error cost function)

Here, we replaced the L2 error term in the cost function by an L1 error term as explained in detail Section 4(A). The results are shown in Fig.7 and Fig.8.

We can see that the small bump (jerk in motion) in Fig.6 has been flattened as shown in Fig.8.

D. Enhancement 2 (Using force-feedback)

Here, we used force-feedback to reduce apparent mass and damping of the human-robot coupled system. The results are shown in Fig.10 and Fig.9.

As compared to the results of the adaptive stiffness, we noticed that we are able to preserve the passivity of the system and able to track the desired trajectory with desired error while allowing appropriate patient participation and also reducing the apparent mass and damping of coupled system.

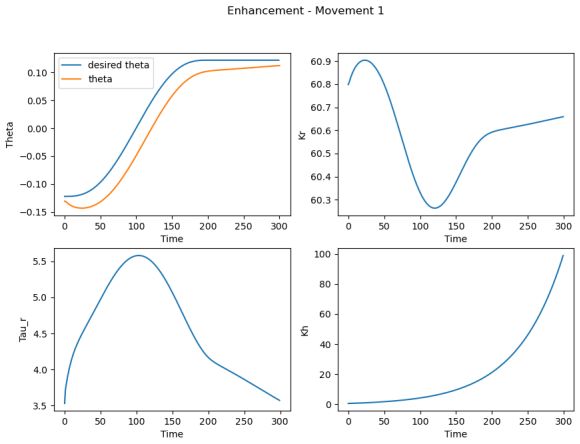

Fig. 7. Plot of a) θ, b) K_r, c) τ_r, and d) K_h for dorsiflexion for Enhancement 1

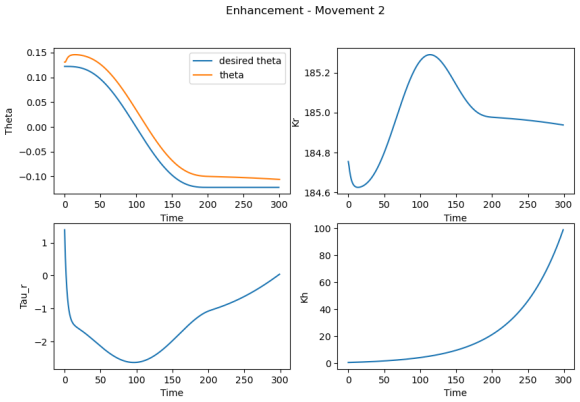

Fig. 8. Plot of a) θ, b) K_r, c) τ_r, and d) K_h for plantarflexion for Enhancement 1

VII. Conclusion

The proposed adaptive impedance control strategy for assistive-resistive robot-aided therapy consists of an iterative process of error-based estimation of the patient's participation and online adaptation of the robotic assistance. We conclude that the advancements we proposed has actually improved the system performance. Like the proposed enhancement 1 has improved the smoothness in motion of the system by reducing sudden jerk (bump) in the dorsi-plantar flexion angle (θ). Also, in proposed enhancement 2, we were able to improve the backdrivability of the system by reducing the overall apparent mass and damping.

Our implementation is available in this **GitHub Repository**

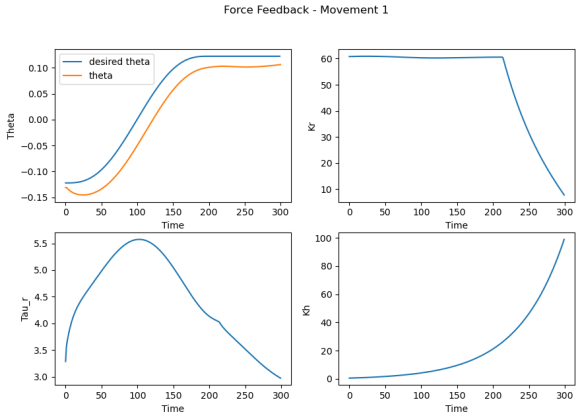

Fig. 9. Plot of a) θ, b) K_r, c) τ_r, and d) K_h for dorsiflexion for Enhancement 2

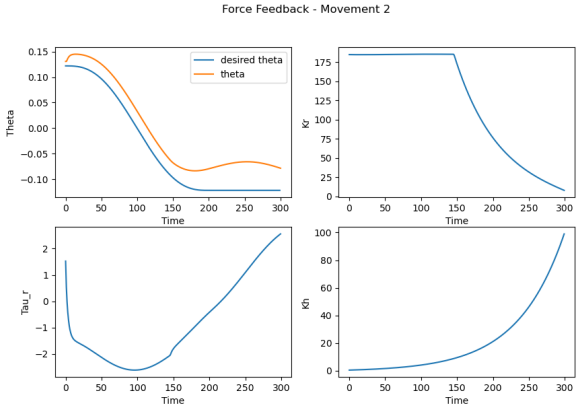

Fig. 10. Plot of a) θ, b) K_r, c) τ_r, and d) K_h for plantarflexion for Enhancement 2

VIII. Future Work

After brainstorming multiple ideas, we had few interestings design enhancements in our mind but due to time constraint we weren't able to implement them. For improvements, we came across couple of resources such as, ankle rehabilitation inside high density fluids as mentioned in [19]. This can encourage the patient to apply more effort due to the damping of the fluid. Also, the system design can be modified to a pedal-like system as mentioned in [20] where the foot is attached to the pedal and the actuator is coupled to the pedal. This system can accomodate wide range of patients since there is no physical constraint for the patient to use this system. The mass of the system doesn't add to load carried by the patient.

References

[1] J. C. Pérez-Ibarra, A. A. G. Siqueira, M. A. Silva-Couto, T. L. de Russo and H. I. Krebs, "Adaptive Impedance Control Applied to Robot-Aided Neuro-Rehabilitation of the Ankle," in IEEE Robotics and Automation Letters, vol. 4, no. 2, pp. 185-192, April 2019, doi: 10.1109/LRA.2018.2885165.

[2] A. Roy, H. I. Krebs, J. E. Barton, R. F. Macko and L. W. Forrester, "Anklebot-assisted locomotor training after stroke: A novel deficit-adjusted control approach," 2013 IEEE International Conference on Robotics and Automation, 2013, pp. 2175-2182, doi: 10.1109/ICRA.2013.6630869.

[3] J. C. Perez Ibarra, W. M. dos Santos, H. I. Krebs and A. A. G. Siqueira, "Adaptive impedance control for robot-aided rehabilitation of ankle movements," 5th IEEE RAS/EMBS International Conference on Biomedical Robotics and Biomechatronics, 2014, pp. 664-669, doi: 10.1109/BIOROB.2014.6913854.

[4] J. C. Pérez-Ibarra, A. A. G. Siqueira and H. I. Krebs, "Assist-as-needed ankle rehabilitation based on adaptive impedance control," 2015 IEEE International Conference on Rehabilitation Robotics (ICORR), 2015, pp. 723-728, doi: 10.1109/ICORR.2015.7281287.

[5] E. J. Rouse, L. J. Hargrove, E. J. Perreault and T. A. Kuiken, "Estimation of Human Ankle Impedance During the Stance Phase of Walking," in IEEE Transactions on Neural Systems and Rehabilitation Engineering, vol. 22, no. 4, pp. 870-878, July 2014, doi: 10.1109/TNSRE.2014.2307256.

[6] A. F. Azocar, A. L. Shorter and E. J. Rouse, "Damping Perception During Active Ankle and Knee Movement," in IEEE Transactions on Neural Systems and Rehabilitation Engineering, vol. 27, no. 2, pp. 198-206, Feb. 2019, doi: 10.1109/TNSRE.2019.2894156.

[7] A. Roy, ENPM640 Lecture Slides, August 2022.

[8] Stroke risk among middle-age increases. [Online]. Available: Link

[9] Concept of stroke by healthline. [Online]. Available: Link

[10] Statistics of stroke by Centers for disease control and prevention. [Online]. Available: Link

[11] K. P. Michmizos and H. I. Krebs, "Assist-as-needed in lower extremity robotic therapy for children with cerebral palsy," in Proc. IEEE RAS EMBS Int. Conf. Biomed. Robot. Biomechatronics: BioRob2012, Rome, 2012, pp. 1081–1086.

[12] Marchal-Crespo and D. J. Reinkensmeyer, "Review of control strategies for robotic movement training after neurologic injury," J. Neuroeng. Rehabil., vol. 6, no. 1, 2009, Art. no. 20.

[13] N.G. Tsagarakis, M. Laffranchi,B. Vanderborght, D.G. Caldwell, "A compact soft actuator unit for small scale human friendly robots," in Proc. of 2009 IEEE Int. Conference on Robotics and Automation,pp.4356-4362.

[14] N. Hogan, "Impedance control: An approach to manipulation," J. Dyn. Syst. Meas. Control, vol. 107, pt. 1–3, no. 1, pp. 1–24, 1985.

[15] H. I. Krebs et al., "Rehabilitation robotics: Performance-based progressive robot-assisted therapy," Auton. Robots, vol. 15, pp. 7–20, 2003.

[16] V. Do Tran, P. Dario, and S. Mazzoleni, "Kinematic measures for upper limb robot-assisted therapy following stroke and correlations with clinical outcome measures: A review," Med. Eng. Phys., vol. 53, pp. 13–31, 2018.

[17] A. Roy et al., "Robot-aided neurorehabilitation: A novel robot for annkle rehabilitation," IEEE Trans. Robot., vol. 25, no. 3, pp. 569–582, Jun. 2009.

[18] Reference for Anthropometric Segment of human body. (Attachment-III Anthromopometry.pdf in UMD CANVAS)

[19] C. H. Guzmán-Valdivia et al., "Design, Development and Control of a Therapeutic Robot Incorporating Aquatic Therapy for Ankle Rehabilitation," Machines, vol. 9, no. 11, p. 254, Oct. 2021, doi: 10.3390/machines9110254.

[20] J. C. Pérez-Ibarra, A. L. Jutinico Alarcón, J. C. Jaimes, F. M. Escalante Ortega, M. H. Terra and A. A. G. Siqueira, "Design and analysis of H_∞ force control of a series elastic actuator for impedance control of an ankle rehabilitation robotic platform," 2017 American Control Conference (ACC), 2017, pp. 2423-2428, doi: 10.23919/ACC.2017.7963316.